The ionization length in plasmas with finite temperature ion sources

N. Jelić,[1] L. Kos,[2] D. D. Tskhakaya, Sr.,[1,3] and J. Duhovnik[2]
[1]*Association EURATOM-ÖAW, Institute for Theoretical Physics, University of Innsbruck,
A-6020 Innsbruck, Austria*
[2]*LECAD Laboratory, Faculty of Mechanical Engineering, University of Ljubljana,
SI-1000 Ljubljana, Slovenia*
[3]*Institute of Physics, Georgian Academy of Sciences, 0177 Tbilisi, Georgia*

The ionization length is an important quantity which up to now has been precisely determined only in plasmas which assume that the ions are born at rest, i.e., in discharges known as "cold ion-source" plasmas. Presented here are the results of our calculations of the ionization lengths in plasmas with an arbitrary ion source temperature. Harrison and Thompson (H&T) [Proc. Phys. Soc. **74**, 145 (1959)] found the values of this quantity for the cases of several ion strength potential profiles in the well-known Tonks–Langmuir [Phys. Rev. **34**, 876 (1929)] discharge, which is characterized by "cold" ion temperature. This scenario is also known as the "singular" ion-source discharge. The H&T analytic result covers cases of ion sources proportional to $\exp(\beta\Phi)$ with Φ the normalized plasma potential and $\beta = 0, 1, 2$ values, which correspond to particular physical scenarios. Many years following H&T's work, Bissell and Johnson (B&J) [Phys. Fluids **30**, 779 (1987)] developed a model with the so-called "warm" ion-source temperature, i.e., "regular" ion source, under B&J's particular assumption that the ionization strength is proportional to the local electron density. However, it appears that B&J were not interested in determining the ionization length at all. The importance of this quantity to theoretical modeling was recognized by Riemann, who recently answered all the questions of the most advanced up-to-date plasma-sheath boundary theory with cold ions [K.-U. Riemann, Phys. Plasmas **13**, 063508 (2006)] but still without the stiff warm ion-source case solution, which is highly resistant to solution via any available analytic method. The present article is an extension of H&T's results obtained for a single point only with ion source temperature $T_n = 0$ to arbitrary finite ion source temperatures. The approach applied in this work is based on the method recently developed by Kos *et al.* [Phys. Plasmas **16**, 093503 (2009)]. © *2009 American Institute of Physics.* [doi:10.1063/1.3271412]

I. INTRODUCTION

The ionization frequency ν_i and likewise the ionization length (L_i) are an important quantity in plasma physics. In investigations into the plasma and sheath problem the importance of this issue is convenient to illustrate on the problem of how to patch quasineutral plasma and collisionless sheath via intermediate scale theory [see, e.g., Riemann 2009 (Ref. 1) and references therein]. Namely, the ionization frequency/length is the basic quantity toward finding the solution of any particular Tonks–Langmuir[2] model (described below in detail). In the theory of intermediate plasma scale used in, e.g., Kaganovich's work,[3] which has been oriented to practical applications, he found an explicit numerical-experimental result expressed in a formula for the electric field where ionization frequency is a quantity to be calculated as an eigenvalue. Note that the ionization frequency in his work was denoted by "Z," while we prefer to use the "classic notation" ν_i.

The Tonks–Langmuir[2] problem of collisionless discharges is old and fairly fundamental in the area of basic plasma physics and application in space laboratory and fusion plasmas. Our mathematical formulation of the problem can be expressed in the form of a general integrodifferential equation

$$\varepsilon^2 n(\Phi) \frac{1}{\Psi^3} \frac{d\Psi}{d\Phi} = 1 - \lambda \int_0^\Phi \Psi(\Phi') \mathcal{K}(\beta, \tau, \Phi', \Phi) d\Phi', \quad (1)$$

where the unknown function to be found is $\Psi(\Phi)$, while other functions, e.g., singular kernel $\mathcal{K}$, and local function $n(\Phi)$ are prescribed in advance, and arbitrary parameters of the problem are β, ε, and τ, while the eigenvalue of problem is λ. The eigenvalue is dependent on the ionization frequency. It depends on the physical model, i.e., particular boundary conditions.

From the physical point of view, Eq. (1) is just the first step to solving a complete elementary problem of the coupled Poisson and Boltzmann equations. While the derivation details of the coupled problem resulting from Eq. (1) will be elaborated below, it should be pointed out here that such an equation emerges from an elementary physical scenario with numerous approximations and compromises but, nevertheless, still remains mathematically so stiff that up to today it has never been solved without considerable additional simplifications.

T&L found that the complete problem can be split into "plasma approximation," where strict quasineutrality is assumed and "sheath approximation" where the electric field dominates. The corresponding two regions of the plasma-wall transition layer are often referred to as "the presheath"

and "the Debye sheath" regions. T&L found approximate solutions for these two regions in plane, cylindrical and spherical geometries. Their "intuitive" approach of splitting the plasma-sheath equation into two parts was later rendered into a precise mathematical context recognized by Caruso and Cavaliere,[4] who employed for this purpose the boundary layer theory by van Dyke. Their approach in application to plasma physics is now known as the "two-scale" plasma and sheath approximation. Following the two-scale approach Harrison and Thompson (H&T) (Ref. [5]) upgraded T&L approximate solution to an exact analytic one; however, holding for the cold ion source distribution under the assumption of strict quasineutrality. Soon after the H&T publication Self[6] announced a complete numerical solution, i.e., with the quasineutrality assumption removed, but still with a singular (cold) ion source. Emmert *et al.*[7] tackled the plasma solution ($\varepsilon=0$) with a regular (warm) ($T_n \neq 0$) but artificial ion source, prepared in advance to yield a Maxwellian ion distribution function. Bissell and Johnson (B&J),[8] however, decided to start from a more realistic, i.e., Maxwellian ion source, and found a numerical solution within a limited range of ion source temperatures. Their model was constrained by their choice of the kernel approximation and polynomial approximation of the model. Soon after B&J work Scheuer and Emmert (S&E) (Ref. [9]) used a better kernel approximation enabling them to find a solution also holding within the range of low ion source temperatures, but, unfortunately, not for relatively "warm" ion sources, which is of high importance to fusion application. After S&E's work, when the numerical method capabilities, libraries and computing resources considerably increased Kos *et al.*[10] have recently managed to employ the exact kernel instead of an approximate one. Kos *et al.* solved the plasma problem with a regular (finite ion-source temperature) Maxwellian ion-source without any restriction regarding the ion temperature; however, for $\varepsilon=0$ and for a commonly adopted assumption of the ionization source profile proportional to the local electron density. The case with various ion sources has so far been solved only for singular ion sources. H&T (Ref. [5]) defined the problem for a rather general ion source strength profile $S_i \sim n_e$ and solved analytically basic cases $\beta=0,1,2$ with $n_e \sim \exp(\beta\Phi)$, (with Φ the normalized local plasma potential) where case $\beta=0$ corresponds to the "flat" ion source spatial distribution (e.g., caused by an electron beam or an external laser-caused ionization), $\beta=1$ corresponds to the single-stage electron-neutral impact ionization and $\beta=2$ assumes two-stage ionization mechanism. The particular numerical value of β (please note that in original H&T work they use another notation for β) can also be an arbitrary positive or negative number providing it can be constructed from a possible physical scenario, which involves volume ion gains and losses. Alternatively, particle-in-cell (PIC) simulations[11] can be employed with no knowledge of β being required. From the theoretical point of view, scenarios with particular β values with combined ionization mechanisms are of considerable importance but can hardly be constructed for a general case, i.e., it is complex enough even for simplified discharges, i.e., even for relatively "clean" physical scenarios $\beta=0,1,2$.

Recently Sternovski *et al.*[12] have tackled the plasma-sheath problem numerically taking into account two source terms of ions, i.e., a homogeneous ionization source and the charge exchange source, both under the assumption of *cold initial velocities* of new born ions. Limiting cases of either charge exchange (collision dominated) and direct external ionization (collision free) were well established and theoretically solved by Riemann.[13] Kuhn *et al.*[14] and Jelić *et al.*[15] also solved these limiting problems numerically and using PIC simulations, for the case of strict quasineutrality and for the special purpose of determining the so-called "ion polytropic coefficient," however. This is a quantity of particular importance to determine the local ion sound velocity. Recently, Robertson[16] made attempts to find a solution of the sheath and presheath in plasmas with warm ion Maxwellian sources for several particular ion source temperatures. His investigation presents a further effort to deal with singularity problems which B&J and S&E have faced. As a particular result he confirmed the results obtained by B&J and S&E regarding the great difference between the initial ion source temperature and the final temperature. Meanwhile Kos *et al.*[10] performed a more detailed research with in an extremely wide range of ion source temperatures, for the $\varepsilon=0$ case with detailed profiles of relevant quantities.

A particular problem of special interest which has never been solved for the finite ion temperature is calculation of the ionization length. While for the case of exponential (proportional to electron density) ion strength H&T obtained their famous single value ≈ 0.405 (i.e., for $T_n=0$) Kos *et al.* recently calculated the whole curve valid for arbitrary ion source temperature T_n, i.e., they solved the problem with $\beta=1$. Analogous solutions with other β values still remain unknown. The main reason is that this is an extremely expensive task. Nevertheless, we made efforts to solve the ionization length problem for another very important case $\beta=0$ (the flat potential profile), for which H&T found the exact value 0.344 for $T_n=0$. Our attention to $\beta=0$ was drawn because of its high importance to various kind of discharges.[12,16,17]

As the main result of the present work we calculate the ionization length L_i for both cases $\beta=0$ and $\beta=1$. So unlike the vanishing ion-source temperature limit the present work finally shows complete dependence of L_i on the arbitrary ion source temperature relevant for a variety of space, laboratory and fusion plasmas. Results are confirmed by means of the PIC simulation method (for further reading on PIC see, e.g., recent work by Tskhakaya *et al.*[11] from 2008 and references therein). Unlike all above-cited numerical works we use an extremely high spatial resolution at the plasma boundaries.

In Sec. II we present theoretical considerations leading to a complete plasma and sheath equation with ionization source strength proportional to $\exp(\beta\Phi)$. In Sec. III we present the numerical procedure. The results are presented in Sec. IV, while Sec. V is a brief summary with discussion and conclusion.
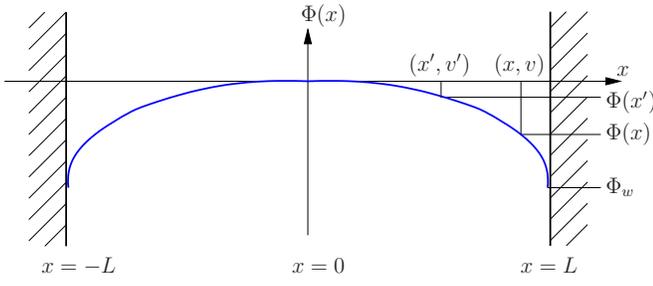
FIG. 1. (Color online) The geometry and coordinate system.

II. THEORETICAL BACKGROUNDS

The general formulation of the problem of the plane-parallel symmetric discharge, as shown in the schematic diagram of problem geometry Fig. 1, consists of simultaneously solving Boltzmann's kinetic equation for ion velocity distribution function (VDF) $f_i(x,v)$,

$$v\frac{\partial f_i}{\partial x} - \frac{e}{m_i}\frac{d\Phi}{dx}\frac{\partial f_i}{\partial v} = S_i(x,v),\tag{2}$$

and Poisson's equation

$$-\frac{d^2\Phi}{dx^2} = \frac{e}{\varepsilon_0}(n_i - n_e).\tag{3}$$

The source term $S_i(x,v)$ on the right-hand side of Eq. (2) describes microscopic processes assumed for a particular scenario of interest, x being the Cartesian space coordinate, v the particle velocity, e the positive elementary charge, m_i the ion mass, $\Phi(x)$ the electrostatic potential at position x, ε_0 the vacuum dielectric constant, and $n_{i,e}$ are the ion and electron densities, respectively. The main subject of the present investigation is the source term $S_i(x,v)$. It can be defined in a fairly general form

$$S_i(v,x) = R n_n n_e(x) f_n\left(\frac{v}{v_{T_n}}\right) H\left(\frac{m_i v^2}{2}\right),\tag{4}$$

where R is the ionization rate, n_n is the density of neutrals with certain VDF (which is in our case uniform over the system) $f_n(v/v_{T_n})$ and the electrons follow Boltzmann distribution $n_e(x) = n_0 \exp(\beta e \Phi(x)/kT_e)$ with n_0 the electron density at $x=0$; $v_{T_n} = \sqrt{kT_n/m_n}$ (it is assumed that for the present investigation the neutral atom mass m_n is equal to the ion mass m_i and $T_n \equiv T_{i,\mathrm{src}}$ is the ion source or, alternatively, the neutral gas temperature), $H(z)$ denotes the Heaviside step function that is introduced to satisfy the positiveness of the kinetic energy of the born ion.

The requirement that the ion current must be equal to the electron current at the wall leads to writing $\Gamma_i = \Gamma_e$ and

$$L R n_n n_{e,\mathrm{av}} = \frac{1}{\sqrt{2\pi}} v_{T_e} n_0 \exp\left(\frac{\beta e \Phi_w}{kT_e}\right),\tag{5}$$

where $n_{e,\mathrm{av}}$ represents the average value of the electron density over the system, $v_{T_e} = \sqrt{kT_e/m_e}$, and m_e, T_e are the electron mass and electron temperature, respectively, while Φ_w is the wall potential as indicated in Fig. 1. The plates in Fig. 1 at $x \pm L$ are assumed to be perfectly absorbing and electri-

cally floating. Although the plates are grounded in an experiment, it is convenient to take the potential of the discharge center as referential, i.e., the electrostatic potential $\Phi(x)$ is assumed to be monotonically decreasing (for $x>0$) and is defined to be zero at $x=0$. With the help of an auxiliary function

$$F_n\left(\frac{v}{v_{T_n}}\right) = \sqrt{2\pi} \cdot v_{T_n} f_n\left(\frac{v}{v_{T_n}}\right),\tag{6}$$

where $v_{T_n} = \sqrt{kT_n/m_n}$ (and it is assumed that for the present investigation the neutral atom mass m_n is equal to the ion mass m_i), the source term in Eq. (4) acquires the form

$$S_i(x,v) = \frac{1}{L} B n_e(x) F_n\left(\frac{v}{v_{T_n}}\right) H\left(\frac{m_i v^2}{2}\right),\tag{7}$$

$$B = \frac{1}{2\pi}\sqrt{\frac{T_e}{T_n}\frac{m_i}{m_e}}\frac{n_0}{n_{e,\mathrm{av}}}\exp\left(\frac{\beta e \Phi_w}{kT_e}\right).\tag{8}$$

Quantity B (originally introduced by B&J) is related to the ionization frequency ν_i, and the characteristic ionization length L_i is

$$\nu_i = B\frac{\sqrt{2\pi}}{L} v_{T_n}, \quad \text{and} \quad L_i = \frac{c_s}{\nu_i} = \frac{L}{B}\sqrt{\frac{T_e}{2\pi T_n}}.\tag{9}$$

The general solution of Eq. (2) with the source term equation (7) is

$$f_i^{\pm}(x,v) = \bar{f}_i^{\pm}\left(v'^2 + \frac{2e}{m_i}\Phi(x')\right) \pm \frac{B}{L}n_0$$
$$\times \int^x \frac{dx'}{\sqrt{v'^2}}\exp\left(\frac{\beta e \Phi(x')}{kT_e}\right) F_n\left(\pm\frac{\sqrt{v'^2}}{v_{T_n}}\right) H(v'^2),\tag{10}$$

where

$$v'^2 = v^2 - \frac{2e}{m_i}\{\Phi(x') - \Phi(x)\}.\tag{11}$$

We remind that the parameter β characterizes the rate of ion generation per unit volume: when $\beta=0$ the rate is uniform; when $\beta=1$ the rate is proportional to the electron density. The values of β greater than unity correspond to those cases where ion generation due to ionization is multiple stage process dependent upon the electron density. In Eq. (10) $f_i^{\pm}$ denotes the VDF of the ions moving in the positive (+) and negative (−) directions of the x-axis ($x>0$), respectively. The point (x',v') in the phase-space (see Fig. 1) is the point of the ion birth. The ion velocity at the observation point we can find from the energy conservation law Eq. (11). Further we consider the symmetric distribution of neutrals, when

$$F_n\left(+\frac{v}{v_{T_n}}\right) = F_n\left(-\frac{v}{v_{T_n}}\right).\tag{12}$$

Functions $\bar{f}_i^{\pm}(x,v)$ are arbitrary functions corresponding to the homogeneous part of Eq. (2) to be constrained by conditions as follows: (a) at the center of the system, $x=0$, the VDF must be symmetric in the velocity space

$[f_i^+(0,v)=f_i^-(0,v)]$ and (b) due to perfect absorption there are no ions at the wall surface, $x=L$, moving with the negative velocity ($f_i^-(L,v)=0$). After straightforward calculations we obtain the following solution of the Boltzmann kinetic equation for the arbitrary distribution function of neutrals:

$$f_i^+(x,v) = B\frac{n_0}{L}\left\{\int_0^x dx' + \int_0^L dx'\right\}F_n\left(+\frac{\sqrt{v'^2}}{v_{T_n}}\right)$$
$$\times\frac{1}{\sqrt{v'^2}}\exp\left(\frac{\beta e\Phi(x')}{kT_e}\right)H(v'), \qquad (13)$$

(where brackets $\{\int\}$ denote integral operator) and

$$f_i^-(x,v) = B\frac{n_0}{L}\int_x^L dx' F_n\left(-\frac{\sqrt{v'^2}}{v_{T_n}}\right)$$
$$\times\frac{1}{\sqrt{v'^2}}\exp\left(\frac{\beta e\Phi(x')}{kT_e}\right)H(-v'). \qquad (14)$$

In Eqs. (13) and (14) the velocity v' is defined by expression Eq. (11). Here it is necessary to mention that the similar solutions are found by Riemann[18] using different from (a) boundary condition [see the boundary condition (a) used by us above].

For the Maxwellian source the auxiliary function Eq. (6) takes the form

$$F_n\left(\frac{v}{v_{T_n}}\right) = \exp\left(-\frac{v^2}{2v_{T_n}^2}\right). \qquad (15)$$

The ion density and the ion flux are moments of velocity distribution which in nondimensional variables read

$$\frac{v}{\sqrt{2}c_s} \rightarrow v, \quad \frac{e\Phi(x)}{kT_e} \rightarrow \Phi(x), \quad \frac{x}{L} \rightarrow x,$$
$$\qquad (16)$$
$$\frac{n_{i,e}}{n_0} \rightarrow n_{i,e}, \quad \frac{\Gamma_{i,e}}{n_0 c_s} \rightarrow \Gamma_{i,e},$$

with auxiliary nondimensional variables

$$\tau \equiv \frac{T_e}{T_n} \rightarrow \frac{1}{T_n}, \quad c_s \equiv \sqrt{\frac{kT_e}{m_i}}, \qquad (17)$$

and with a nondimensional quantity of central interest, as appeared in a natural manner above

$$\frac{L_i}{L} = \frac{1}{B\sqrt{2\pi T_n/T_e}} \rightarrow L_i. \qquad (18)$$

At this place we have to remind that the normalization is a matter of taste up to multiplicative constant, as somehow pointed out by Sternovsky *et al.*[12] in their list of references. In this we have to keep in mind that the definition Eq. (18) is adjusted to "taste" of H&T, but can be converted in a trivial manner to, e.g., according to works of Riemann (see, e.g., Refs. 1 and 19) via multiplying by a factor of $\sqrt{2}$.

The density and in flux for the Maxwellian source now take the form

$$n(x) = 2B\int_0^\infty dv \int_0^1 dx' \exp[\beta\Phi(x')]$$
$$\times\frac{\exp\{-\tau[v^2-\Phi(x')+\Phi(x)]\}}{\sqrt{v^2-\Phi(x')+\Phi(x)}}$$
$$\times H[v^2-\Phi(x')+\Phi(x)], \qquad (19)$$

$$\Gamma(x) = 2\sqrt{2}B\int_0^\infty v dv \int_0^1 dx' \exp[\beta\Phi(x')]$$
$$\times\frac{\exp\{-\tau[v^2-\Phi(x')+\Phi(x)]\}}{\sqrt{v^2-\Phi(x')+\Phi(x)}}$$
$$\times H[v^2-\Phi(x')+\Phi(x)]. \qquad (20)$$

The integral over x' in Eq. (19) can be split into two parts

$$\int_0^1 dx'(\cdots) = \int_0^x dx'(\cdots) + \int_x^1 dx'(\cdots). \qquad (21)$$

In the first interval $(0,x)$ of the integration we see that $\Phi(x')-\Phi(x)\geq 0$ holds, and in the second $\Phi(x')-\Phi(x)\leq 0$. This allows us to use the cutoff property of the *H*-function and finally we find

$$n(x) = B\int_0^1 dx' \exp[\beta\Phi(x')]$$
$$\times\exp\left[\frac{\tau}{2}\{\Phi(x')-\Phi(x)\}\right]K_0\left(\frac{\tau}{2}|\Phi(x')-\Phi(x)|\right), \qquad (22)$$

with

$$\Gamma(1) = \sqrt{\frac{2\pi}{\tau}}B\int_0^1 dx' \exp[\Phi(x')]. \qquad (23)$$

In obtaining Eq. (22), the relation

$$2\int_0^\infty \frac{\exp(-\tau x^2)}{\sqrt{x^2+a^2}} = \exp\left(\frac{\tau}{2}a^2\right)K_0\left(\frac{\tau a^2}{2}\right), \qquad (24)$$

with $K_0(z)$ the modified Bessel function of zeroth order was employed. Equation (22) coincides with the expression for the ion density used in Refs. 8 and 9. In the limit of the cold source $T_n\rightarrow 0$, where the auxiliary function reads $F_n(v/v_{T_n})=\sqrt{2\pi}v_{T_n}\delta(v)$ [$\delta(z)$ is the Dirac δ-function], we find the expression for the ion density

$$n(x) = \frac{1}{\sqrt{2}}\int_0^x \frac{dx'}{L_i}\frac{\exp[\Phi(x')]}{\sqrt{\Phi(x')-\Phi(x)}}, \qquad (25)$$

discussed previously in detail in Refs. 20 and 21. In Eq. (25) L_i is defined by Eq. (9). In the dimensionless form Poisson's Eq. (3) finally acquires the form

$$\frac{1}{B} = \frac{1}{1 - \exp(-\Phi)\varepsilon^2 \dfrac{d^2\Phi}{dx^2}}$$

$$\times \int_0^1 dx' \, \exp\left[\left(\beta + \frac{\tau}{2}\right)\Phi(x') - \left(1 + \frac{\tau}{2}\right)\Phi(x)\right]$$

$$\times K_0\left(\frac{\tau}{2}|\Phi(x') - \Phi(x)|\right), \tag{26}$$

where $\varepsilon = \lambda_D / L$ with the electron Debye length $\lambda_D = \sqrt{\varepsilon_0 kT_e/(e^2 n_0)}$. In fact ε represents the measure of the quasineutrality degree.

In Eq. (26) we have replaced the original H&T notation of the ionization profile $\exp(\gamma e\Phi/kT_e)$ with $\exp(\beta e\Phi/kT_e)$, as the coauthors of the present work use the γ symbol as exclusive notation for the "polytropic" coefficient (see, e.g., Refs. 14 and 15). Using Eqs. (5) and (23) to find the floating potential of the wall we use the relation

$$\exp(\Phi_w) = 2\pi \sqrt{\frac{m_e}{m_i}} \sqrt{\frac{T_n}{T_e}} B \int_0^1 dx' \, \exp[\Phi(x')]. \tag{27}$$

After introducing quantity $\Psi \equiv dx/d\Phi$, it is now a straightforward task to derive mathematical expression given by Eq. (1) as applied to a particular class of kernel. Equation (26) describes the potential profile for the arbitrary temperature of the ion sources. The form (1) is mathematically elegant because all unknown and known functions are explicit. Although this is a complex and unclassified type of integral equation,[22] in the limit of $\varepsilon = 0$ it is reduced to a familiar Fredholm type of equation. This appeared to be a natural way followed by B&J to solve the problem starting from the Fredholm type form. However, they applied an intricate method with an approximate kernel which constrained the solution to a rather narrow range of validity. S&E (Ref. 9), however, applied another form without introducing auxiliary function Ψ (which is in fact the inverse electric field with a negative sign). In the S&E form all the functions are implicit, so this form cannot be regarded as the Fredholm type at all but rather as a Hammersteinian equation. Since S&E used a better kernel approximation and used the straightforward method of numerical solution, they obtained results which are valid within a wider range of ion-source temperatures, however, still limited for relatively low values. The problem was finally solved by Kos et al. via employing the exact kernel; however, still only for the particular ionization strength profile proportional to the electron density.

The generalized equation derived which includes a variety of source strength profiles being the exponential function of the potential profile powered by β Eq. (26) is a complex one which is not classified in the mathematical sense at all. A would-be solution of such an equation should yield a full plasma and sheath solution, i.e., the potential profile between the electrodes for a variety of physical scenarios. However, such an equation has never been solved satisfactory without
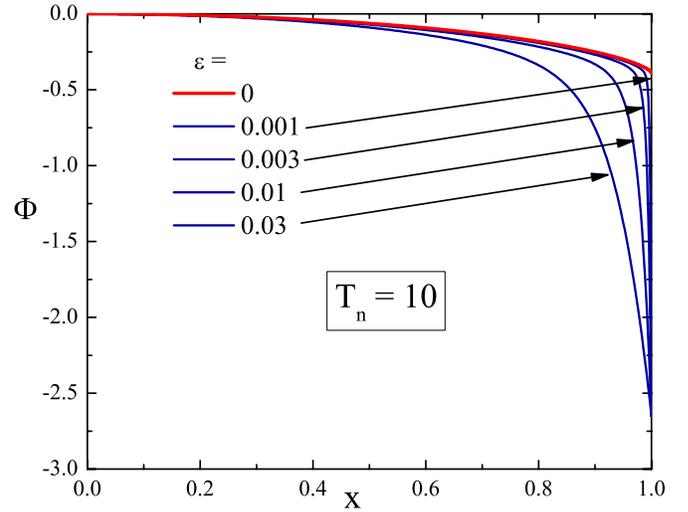
FIG. 2. (Color online) Our preliminary solution with both finite epsilon and finite ion-source temperature plasma-sheath equation of the type equation (26) for $\beta = 1$.

either the $\varepsilon = 0$ assumption or the $1/\tau \equiv T_n = 0$ approximation. We are intensely working on the solution of Eq. (1) for arbitrary ion source. However, this is not a trivial task. In this manuscript we illustrate our preliminary results of finite epsilon finite ion-source temperature plasma-sheath equation of the type equation (26) for $\beta = 1$ (Fig. 2). Unfortunately it turns out that the problem plasma-sheath problem is numerically much more demanding that the two scale approximation. We will solve this problem with a high resolution during our forthcoming investigations.

The most usual practice which is well exhausted by numerous plasma physicists is to consider the approximation with both $T_n = 0$ and $\varepsilon = 0$. Moreover, the usual praxis is further to ignore any other β which is different from one. However, during several couple of decades has been recognized that the plasma and sheath can be patched via so-called intermediate scale analysis (see, e.g., Riemann's[21] work and references therein). For such an approach it is of crucial importance to know the exact values of the plasma potential at the plasma the plasma-sheath boundary as emerges from the two-scale model, as well as the ionization lengths which differ from the physical lengths, as shown above. For finite ion-source temperatures such values became available with recent work of Kos et al.,[10] however, for $\beta = 1$. Since we are aware of particular scientific and practical importance of other scenarios characterized by β values, we performed at the extent possible numerical calculations for the second prominent case, i.e., $\beta = 0$, which correspond to the flat ionization source strength profile over the discharge. Here we consider the $\varepsilon = 0$ approximation, but unlike previous works we deal with finite T_i of arbitrary value. Thus instead of obtaining a single value for $T_i = 0$ such as in H&T,[5] we obtain the whole curve as further described. In addition the results with $\beta = 1$ were again calculated via using upgraded program package which guaranties high reliability of results obtained for either value of β.
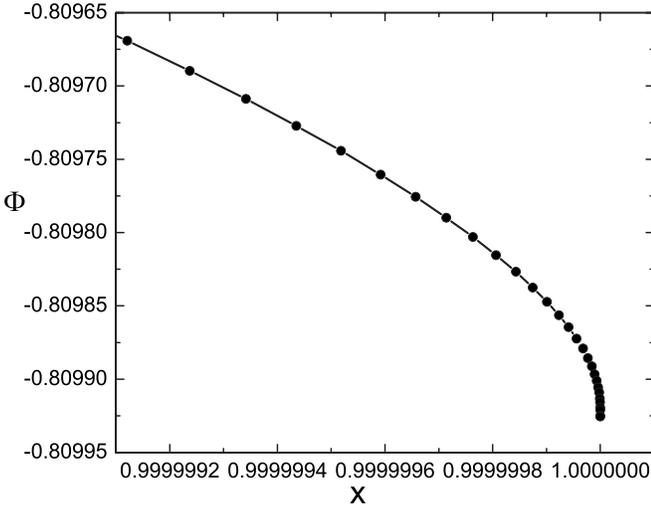
FIG. 3. Last 28 points of the potential profile for $T_n=0.1$, $\beta=1$ with $N=2401$ points and grid density $\lambda_1=1$ and $\lambda_2=2.4$.

III. NUMERICAL METHOD

We solve Eq. (26) numerically in the limit $\varepsilon=0$ when this equation reduces to the Fredholm type integrodifferential equation with a singular kernel and nonlinear function related to Poisson equation (3). Solution function $\Phi(x)$ is known to be smooth and monotonous, having the end point singularity when $\varepsilon=0$. Additionally, Eq. (26) contains unknown constant B, which represents the "eigenvalue" of the system. As has been elaborated by Kos *et al.*[10] the singular behavior at the boundaries of interval $[0,1]$ can be taken into account by using nonuniform grids with increasing density when approaching the singularity.

We introduce the following node positions for N points of the system

$$x_i = [1 - [1 - i/(N-1)]^{\lambda_2}]^{\lambda_1}, \quad i = 0,1,\ldots,N-1, \quad (28)$$

where λ_1 and λ_2 control the density at each boundary. For illustrating our high resolution method with in Fig. 3 we show a zoom of the potential profile at the end of the system obtained with 2401 grid nodes case. Calculating even such a single profile is a very expensive a computational task.

Rearranging Eq. (26) into a form suitable for an iterative procedure and discretizing it into subintervals we obtain

$$\exp\left[\left(1+\frac{1}{2T_n}\right)V_k\right]$$

$$= B\sum_{i=0}^{N-1}\int_{x_i}^{x_{i+1}} dx' \exp\left[\left(\beta+\frac{1}{2T_n}\right)V(x')\right]$$

$$\times K_0\left(\frac{1}{2T_n}|V(x')-V_k|\right). \quad (29)$$

Each node value V_k is also a source for a diagonal singularity in the kernel $K_0(z)$ (a singularity as $x' \to x_k$). In practice, the computation on strongly graded grids may be unstable since the grid points may be located too close to each other near the boundaries, and the system of equations may become rapidly ill-conditioned with increasing λ_1, λ_2, and N. Integra-
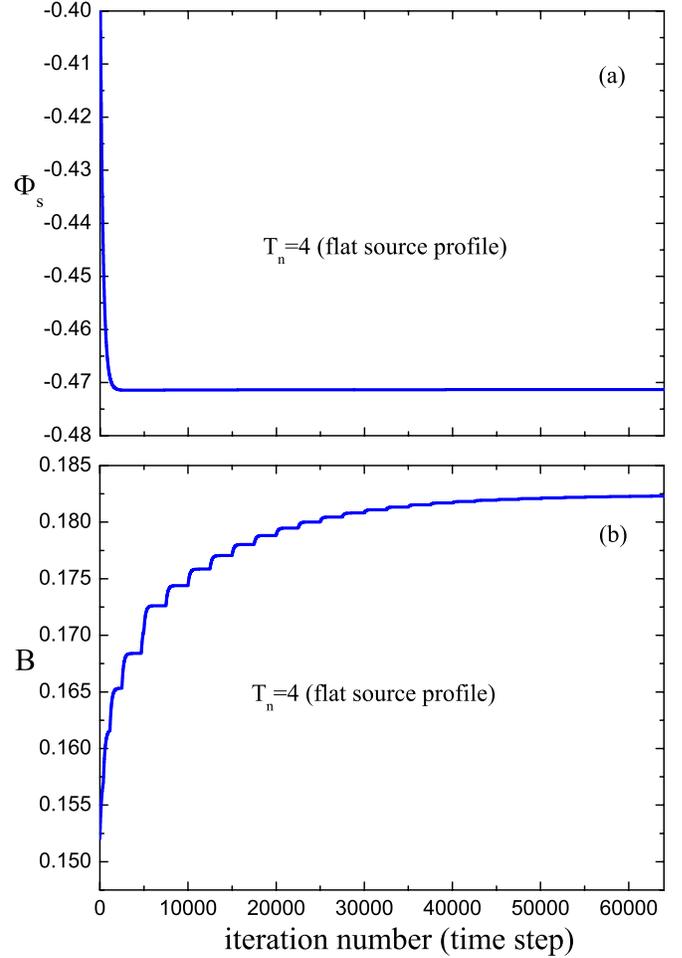
FIG. 4. (Color online) Convergence plots for $T_n=4$ and flat source: (a) Boundary point Φ_s and (b) eigenvalue B.

tion of Eq. (29) in the subintervals is performed directly with adaptive quadrature algorithms[23,24] that we extended to 128-bit quad precision floating point values for increased precision and stability on highly graded grids.

We refer to Ref. 10 for details. In this work we extend the applicability domain of this technique to $\varepsilon=0$ and $\beta=0$. To overcome stability problems we introduced piecewise Lagrangian polynomial interpolation[25] of order two and three in subintervals with small Φ gradients. Although such approximation is often considered to be too expensive for numerical computation, it possesses beautiful symmetry and with a modified (weighted) form is comparable in speed to other approximations. Additionally, we found that the solution for $\beta=0$ (flat ion-source profile) is surprisingly stiffer than for $\beta=1$. This could be due to the imbalance in $\exp(z)$ functions on both sides of Eq. (29). The shifting of the whole solution for $-V_0$ was required to speed up convergence, as shown in Fig. 4, where we illustrate the diagnostic the new results obtained in the present investigation with $\beta=0$ procedure of obtaining "saturated" solution. The staircase effect in Fig. 4(b) is just an illustration of a local convergence when shifting to the origin is not performed within dense intervals. Such behavior was not observed for $\beta=1$. Figure 4(a) shows that end point value Φ_s converges faster than B. An addi-
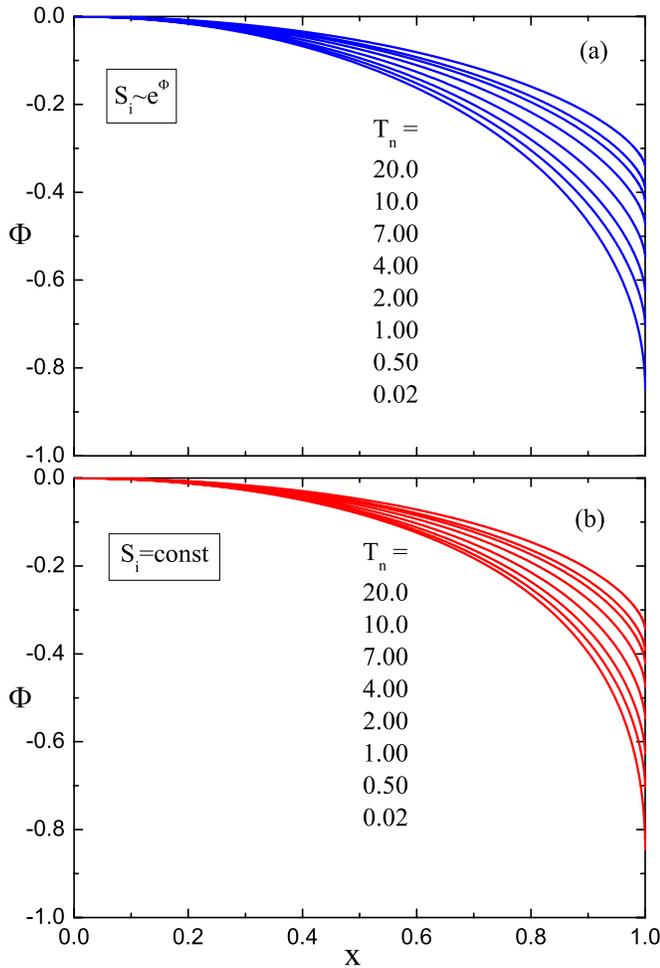
FIG. 5. (Color online) Comparison of potential profiles for (a) Boltzmannian ion source distribution and (b) constant ion source distribution.

tional advantage of our program package is the feature of automatic checking of the convergence criterion for both Φ_s and B. The results are presented in Sec. IV.

IV. RESULTS

In Fig. 5 we show the results of a huge number of calculations performed with our program package to obtain results with various ion source spatial distribution. In addition we employ also the PIC method and perform some simulations in order to check out our results. In Fig. 5 (also in Figs. 8 and 9) the notation $(T_n/T_e) \rightarrow T_n$ is used.

In Fig. 5(a) we show the "classic" set of results obtained in the same manner as by Kos *et al.*[10] for the case $\beta=1$; however, with an upgraded version of the program package, while in Fig. 5(b) we show the case $\beta=0$. Whereas Fig. 5 is employed for a qualitative comparison of alternative ion source profiles and for many ion source temperatures, for more quantitative comparison we select curves obtained for $T_n=1$ and in Fig. 6 we show a comparison of the results. First, there is the potential profile obtained with the classic ion source distribution as employed by B&J (Ref. 8) in comparison with our calculations with $\beta=1$. In fact there is nothing especially new regarding excellent agreement between these two curves since this agreement has already been
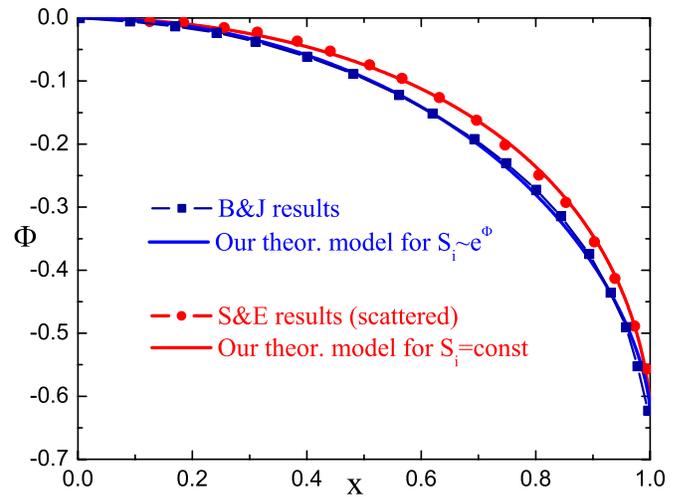
FIG. 6. (Color online) Comparison between B&J (Ref. 8) (scattered squares) and our analytic-numerical model (solid line) and between S&E (Ref. 9) (scattered circles) and our analytic-numerical method for the flat ion-source.

shown by Kos *et al.*[10] Here we only repeat the calculation and show the result. The new material is a comparison of S&E's result as scanned from their article[9] with the result obtained in our present investigation with a constant ion source. S&E claim that their potential profile in their Fig. 1 (Ref. 9) is obtained for the case $\beta=1$. However, we clearly demonstrate that this potential profile corresponds to the case $\beta=0$. This appears to be a coincidence. The coincidence is resolved by means of the PIC simulation method and run for the flat ion source ($\beta=0$). In Fig. 7 our constant ion source results are compared to S&E's scanned results. In Fig. 8 S&E's scanned results are replotted and compared to our PIC simulation results. Again, this method confirms that S&E corresponds to $\beta=0$ and *not* to $\beta=1$ case, as S&E claimed in their work. Note that the deviation of the results appears near the edge of the computational system, where the two models essentially differ since the PIC method can never be reduced to quasineutral plasma, i.e., the sheath region is inherently
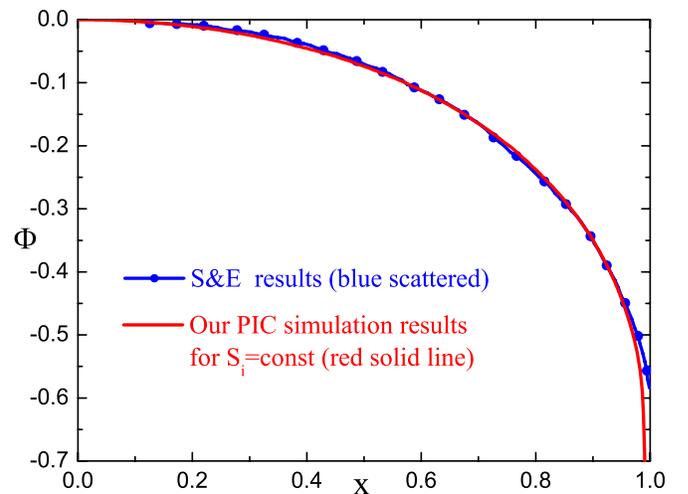
FIG. 7. (Color online) Comparison of S&E's results (scattered line) with our PIC simulation (solid line).
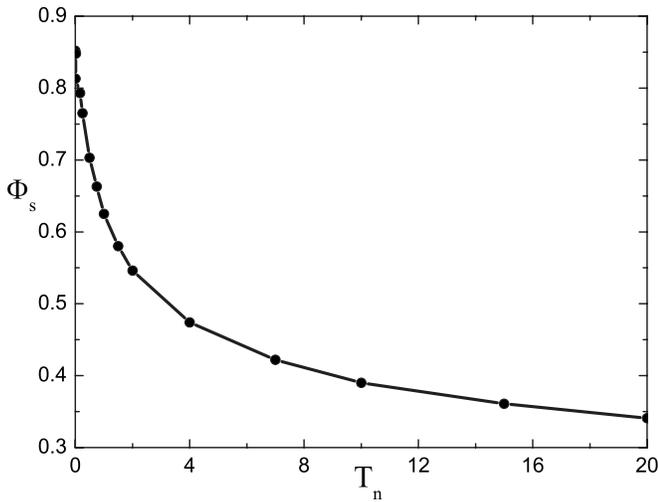
FIG. 8. Boundary potential Φ_s dependency on the normalized ion-source temperature T_n. It is not possible to distinguish between the results obtained for two alternative ion source strength profiles within the drawing accuracy.

present in PIC simulations such as in nature, i.e., real experiments. Comparison with a model with finite ε plasma corresponding such a PIC simulation will be done in a subsequent investigation.

It turns out definitely that S&E in fact worked with the constant ion source and NOT with the source proportional to the electron density. The question arises why their results at the plasma boundary are in such excellent agreement with B&J and Kos *et al.* The present work gives a straightforward answer to this question: it turns out that the plasma parameters at the boundary are invariant to the ionization source profile. Figure 8 shows, e.g., the plasma potential at the point of the electric field singularity. The difference between the cases corresponding to either of above sources is so small (at the third or fourth digit) that it could not be detected within the drawing accuracy at all. In fact, from theoretical point of view there might not be *any* difference, i.e., if it appears this is the problem of numerical calculations. This result confirms
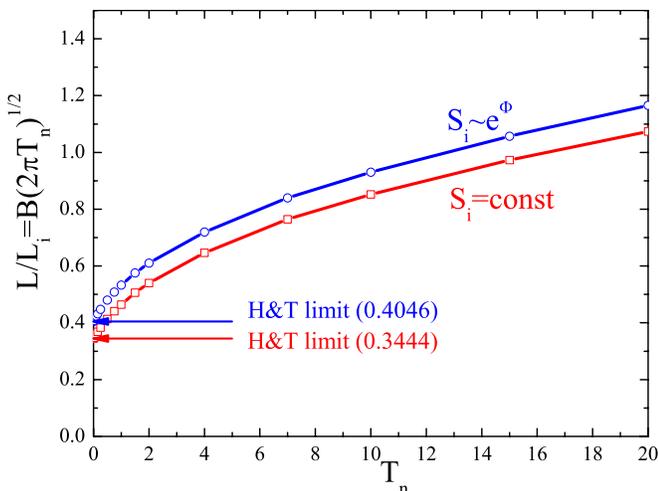
FIG. 9. (Color online) The relation between the ionization length L_i and the length of the system L for two alternative ionization mechanisms as defined by H&T (Ref. 5).
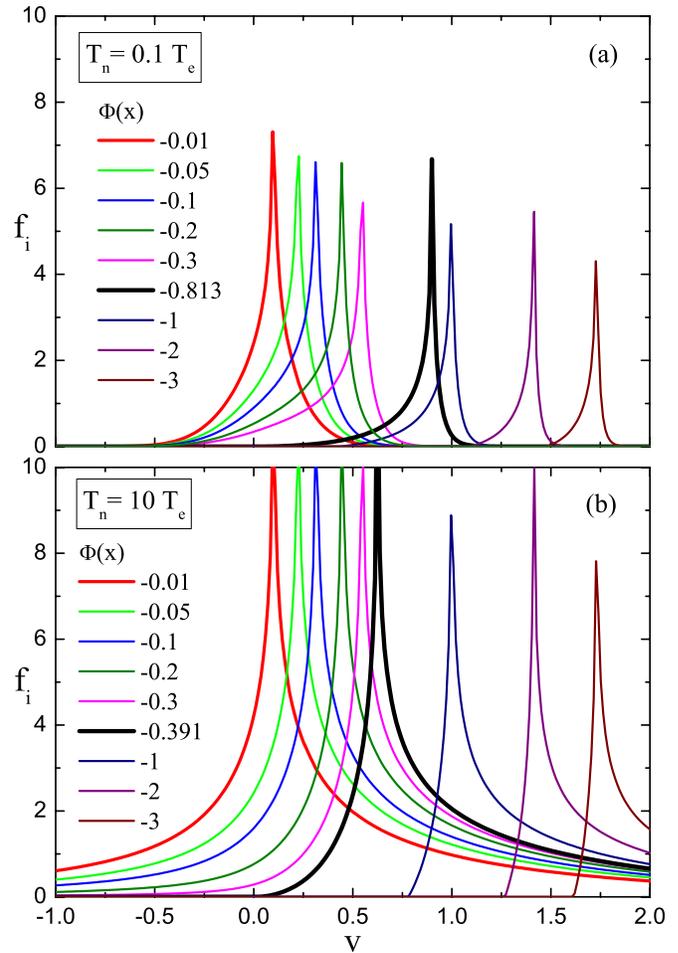
FIG. 10. (Color online) Velocity distributions for (a) $T_n=0.1T_e$ and (b) $T_n=10T_e$.

the theoretical predictions. This concerns only the last point, the profiles, however are dependent on ionization strength profiles.

Figure 9 represents the dependence of the characteristic ionization length Eq. (9) on the ion-source temperature. Both results obtained for the two alternative source profiles are presented in parallel. The curve for $\beta=1$ is our present result performed for the numerical refinement calculation of the result which has already been reported by Kos *et al.*,[10] the novelty being the fact that the very curve for $\beta=0$ is a new one.

While in both cases $\beta=0$ and $\beta=1$ the results have been known only for cold ion sources (single points for $T_i=0$ at our curves) over the last few decades, our results extend to any ion-source (e.g., neutral) temperature. In Fig. 10 ion velocity distribution is shown at various observing points $[\Phi(x)$ on the right side of the discharge] for two distinct ion-source (neutral gas) temperatures. The first one [Fig. 10(a)] corresponds to classic laboratory investigations, while the second one [Fig. 10(b)] is applicable to fusion relevant plasmas. In both figures [(a) and (b)] plasma boundaries $\Phi_s(x_s)$ are marked in bold solid lines. It is evident that ion velocity distribution at those particular points "suddenly" lacks ions with negative ion velocities. This observation should be redefined as a new plasma-sheath criterion in near future. In

fact, this was already been done to some extent by Block and Fälthammar[26] via their criterion for double layer formation existence.

V. DISCUSSION AND CONCLUSION

Our investigation covers a wide range of ion-source temperatures for $\beta = 0$ (so-called flat ion source strength distribution). In fact this is the first investigation using the analytic-numerical method for the finite ion-source temperature with flat ion-source strength distribution. Other methods assume employment of, e.g., the PIC method. In the present work the PIC simulation was used only for the purpose of confirming our doubts on some work done in past, in particular to find out how S&E (Ref. 9) found their potential curve, i.e., why it differed considerably from the curves obtained by S&E and Kos *et al.*[10] We resolved the problem via our numerical computations. Nevertheless we performed additional PIC simulations to confirm our findings. Findings regarding the S&E curve in fact are not of crucial importance to plasma physics, but we feel obliged to resolve the problem for the sake of scientific justice.

Our main result is obtaining the ionization length for an arbitrary ion temperature (Fig. 9) and for different ionization strength profiles. A particular case of the flat ionization profile ($\beta = 0$) is elaborated in details. Calculations with the classic B&J (Ref. 8) model for the ionization source proportional to the electron local density ($\beta = 1$) are performed with increased accuracy and presented in comparison to a flat ion source. It emerges that the plasma-sheath boundary potential Φ_s is *invariant* on the particular ionization profile choice. The detailed profiles and the ionization lengths, on the contrary, are *not* invariant on the particular potential profile choice. The dependence of the ionization length on the ion-source (neutral gas) temperature is investigated in detail for both flat and Boltzmann-distributed ionization sources. While in both cases $\beta = 0$ and $\beta = 1$ the results have only been known for the cold ion sources (single points for $T_i = 0$ at our curves) for the last several decades, our new results embrace any ion-source temperature. Finding the ionization length for a particular ionization source profile with a finite temperature is a task of fundamental importance in plasma physics, especially as a prerequisite for the intermediate plasma-sheath region solution.

The results for arbitrary ε and arbitrary ion source temperatures obtained by Robertson[16] may serve for some particular purposes. However, in order to obtain highly reliable results it is necessary to employ high density grids and apply various algorithms showing the invariance of results as the grid density is increased. For finite ε such results are still missing because of the demanding computations. The present work establishes a good basis toward solving this task.

[1] K.-U. Riemann, Plasma Sources Sci. Technol. **18**, 014006 (2009).
[2] L. Tonks and I. Langmuir, Phys. Rev. **34**, 876 (1929).
[3] I. D. Kaganovich, Phys. Plasmas **9**, 4788 (2002).
[4] A. Caruso and A. Cavaliere, Nuovo Cimento **26**, 1389 (1962).
[5] E. R. Harrison and W. B. Thompson, Proc. Phys. Soc. London **74**, 145 (1959).
[6] S. A. Self, Phys. Fluids **6**, 1762 (1963).
[7] A. Emmert, R. M. Wieland, A. T. Mense, and J. N. Davidson, Phys. Fluids **23**, 803 (1980).
[8] R. C. Bissell and P. C. Johnson, Phys. Fluids **30**, 779 (1987).
[9] J. T. Scheuer and G. A. Emmert, Phys. Fluids **31**, 3645 (1988).
[10] L. Kos, N. Jelić, S. Kuhn, and J. Duhovnik, Phys. Plasmas **16**, 093503 (2009).
[11] D. Tskhakaya, S. Kuhn, Y. Tomita, K. Matyash, R. Schneider, and F. Taccogna, Contrib. Plasma Phys. **48**, 121 (2008).
[12] Z. Sternovsky, K. Downum, and S. Robertson, Phys. Rev. E **70**, 026408 (2004).
[13] K.-U. Riemann, Phys. Fluids **24**, 2163 (1981).
[14] S. Kuhn, K.-U. Riemann, N. Jelić, D. D. Tskhakaya, Sr., D. Tskhakaya, Jr., and M. Stanojević, Phys. Plasmas **13**, 013503 (2006).
[15] N. Jelić, K.-U. Riemann, T. Gyergyek, S. Kuhn, M. Stanojević, and J. Duhovnik, Phys. Plasmas **14**, 103506 (2007).
[16] S. Robertson, Phys. Plasmas **16**, 103503 (2009).
[17] Z. Sternovsky, Plasma Sources Sci. Technol. **14**, 32 (2005).
[18] K.-U. Riemann, private communication (2009).
[19] J. E. Allen, Plasma Sources Sci. Technol. **18**, 014004 (2009).
[20] K.-U. Riemann, J. Phys. D **24**, 493 (1991).
[21] K.-U. Riemann, Phys. Plasmas **13**, 063508 (2006).
[22] A. D. Polyanin and A. V. Manzhirov, *Handbook of Integral Equations*, 2nd ed. (Chapman and Hall, London/CRC, Cleveland, 2008).
[23] R. Piessens, E. de Doncker-Kapenga, C. W. Uberhuber, and D. K. Kahaner, *Quadpack. A Subroutine Package for Automatic Integration*, Series in Computational Mathematics 1 (Springer-Verlag, Berlin, 1983).
[24] M. Galassi, J. Davies, J. Theiler, B. Gough, G. Jungman, M. Booth, and F. Rossi, *Gnu Scientific Library: Reference Manual* (Network Theory, United Kingdom, 2009).
[25] G. Dahlquist and A. Björck, *Numerical Methods in Scientific Computing* (SIAM, Philadelphia, PA, 2008), p. 367.
[26] L. P. Block and C.-G. Fälthammar, Ann. Geophys. **32**, 161 (1976).